ELSEVIER

Biochemical Pharmacology 62 (2001) 283–296

Biochemical Pharmacology

Protection against glutamate toxicity through inhibition of the p44/42 mitogen-activated protein kinase pathway in neuronally differentiated P19 cells

Elfrida R. Grant, Monica A. Errico, Stuart L. Emanuel, Daniel Benjamin, Michael K. McMillian, Scott A. Wadsworth, Robert A. Zivin*, Zhong Zhong[1]

Drug Discovery, R.W. Johnson Pharmaceutical Research Institute, 1000 Route 202 South, Raritan, NJ 08869, USA

Received 26 July 2000; accepted 31 October 2000

Abstract

Excessive levels of the neurotransmitter glutamate trigger excitotoxic processes in neurons that lead to cell death. *N*-Methyl-D-aspartate (NMDA) receptor over-activation is a key excitotoxic stimulus that leads to increases in intracellular calcium and activation of downstream signaling pathways, including the p44/42 mitogen-activated protein (MAP) kinase pathway. In the present study, we have demonstrated that 1,4-diamino-2,3-dicyano-1,4-bis[2-aminophenylthio]butadiene (U0126), a potent and selective inhibitor of the p44/42 MAP kinase signaling pathway, prevents glutamate-induced death in neuronally differentiated P19 cells. In addition, we show that differentiated, but not undifferentiated, P19 cells expressed zeta1, epsilon1, and epsilon2 subunits of the NMDA receptor. Differentiated P19 cells exhibited specific NMDA receptor binding and intracellular calcium responses to glutamate that were blocked by the selective NMDA receptor antagonist [5*R*,10*S*]- [+]-5-methyl-10,11-dihydro-5*H*-dibenzo[a,d]cyclohepten-5,10-imine (MK-801), but not U0126. Glutamate treatment of differentiated P19 cells triggered a rapid and sustained induction in p42 MAP kinase phosphorylation that was blocked by U0126. Pretreatment of differentiated P19 cells with U0126, but not other classes of protein kinase inhibitors, protected against glutamate-induced cell death. Post-treatment with U0126, even as late as 6 hr after glutamate application, also protected against glutamate toxicity. These results suggest that the p44/42 MAP kinase pathway may be a critical downstream signaling pathway in glutamate receptor-activated toxicity.

Keywords: N-Methyl-D-aspartate; Glutamate; p44/42 MAP kinase; Neuroprotection; U0126; Phosphorylation

1. Introduction

Glutamate, the major fast excitatory neurotransmitter in the mammalian central nervous system, depolarizes neurons by opening three classes of ligand-gated ion channels: AMPA, AMPA/kainate, and NMDA receptors. Transient increases in synaptic glutamate levels occur during normal excitatory transmission. On the other hand, excessive increases in synaptic glutamate levels are toxic to neurons, and trigger the process of neuronal cell death commonly referred to as glutamate excitotoxicity [1]. Glutamate excitotoxicity contributes to ischemia-induced brain damage, epilepsy, and various chronic neurodegenerative diseases [1].

Of the three classes of glutamate-gated channels, specific over-activation of the NMDA receptor is primarily responsible for triggering excitotoxic death in a variety of neuron types [1]. In animal stroke models, ischemia-induced brain damage can be largely alleviated by pretreatment with the specific NMDA receptor antagonist [5*R*,10*S*]-[+]-5-methyl-10,11-dihydro-5*H*-dibenzo[a,d]cyclohepten-5,10-imine (MK-801) [2]. In many types of neurons, glutamate

* Corresponding author. Tel.: +1-908-704-4882; fax: +1-908-526-7118.

E-mail address: rzivin@prius.jnj.com (R.A. Zivin).

[1]Current address: Drug Discovery Technologies, Cell & Molecular Technologies, Inc., 580 Marshall St., Phillipsburg, NJ 08865. Tel.: +1-908-454-7774; fax: +1-908-859-6437. *E-mail address:* zzhong@cmt-inc.net

Abbreviations: AMPA, (±)-α-amino-3-hydroxy-5-methylisoxazole-4-propionic acid; NMDA, *N*-methyl-D-aspartate; MAP, mitogen-activated protein; ERK1/2, extracellular signal regulated kinase 1/2; MEK, mitogen-activated protein kinase kinase; JNK, Jun N-terminal kinase; NO, nitric oxide; CDK1, cyclin-dependent kinase I; PKA, protein kinase A; PKC, protein kinase C; CK1/2, casein kinase 1/2; EGFR, epidermal growth factor receptor; CaM-K, calcium/calmodulin-dependent kinase; ATRA, all-*trans*-retinoic acid; RT–PCR, reverse transcriptase–polymerase chain reaction; and CFDA, carboxyfluorescein diacetate.

0006-2952/01/$ – see front matter
PII: S0006-2952(01)00665-7

excitotoxicity is thought to result primarily from an excessive influx of calcium ions due to the high permeability of the NMDA receptor for calcium [3]. High intracellular calcium levels may lead to over-activation of calcium-regulated enzymes such as NO synthase, phospholipases, proteases, and kinases, and may mediate excitotoxicity.

Glutamate signaling through the NMDA receptor induces phosphorylation and activation of MAP kinases in primary neuronal cultures [4,5]. Animal models of ischemic brain injury suggest that increased activity of MAP kinase family members may mediate neuronal injury [6,7]. Deletion of Jnk3, a member of the JNK family of MAP kinases that is expressed predominantly in the brain, protects hippocampal neurons from kainic acid-induced excitotoxicity *in vivo*, although the role of the NMDA receptor in this form of toxicity is not clear [8]. Specific inhibition of the upstream activating kinases of ERK1/2 (p44/42) MAP kinase protects against neuronal damage due to focal cerebral ischemia [7]. In cultured primary hippocampal neurons, inhibition of the ERK1/2 (p44/42 MAP kinase) signaling pathway protects against neuronal death induced by removal of kynurenate, a broad spectrum glutamate-receptor antagonist [9]. Non-receptor-mediated, glutamate-induced oxidative toxicity is also blocked by inhibition of the ERK1/2 signaling pathway [10]. Collectively, these reports clearly indicate an important role for ERK1/2 MAP kinase signaling in glutamate-induced neuronal toxicity. In the present study, we have examined whether the importance of downstream MAP kinase signaling can be demonstrated in the neuronally differentiated P19 cell-line model of NMDA receptor-dependent glutamate excitotoxicity [11]. Verification of the relevance of MAP kinase signaling in this cell culture model would (a) further validate the model system, (b) link NMDA receptor stimulation to MAP kinase activation during excitotoxicity, and (c) establish a simple, homogeneous system in which to identify important glutamate signaling intermediates. Results obtained in neuronally differentiated P19 cells, when confirmed in primary neuronal culture and in *in vivo* animal models, can help identify novel therapeutic targets, and make it possible to set up large scale cell-based compound screens for neuroprotective agents.

P19 cells are a pluripotent embryonal carcinoma line that can be induced to differentiate into post-mitotic neuron-like cells in the presence of high doses of retinoic acid [12,13]. Differentiated P19 cells express a wide variety of neuron-specific markers, as well as a diversity of functional ion channels and receptors [11,14]. Among these are functional NMDA receptors that exhibit NMDA-induced electrophysiological currents that are appropriately sensitive to selective NMDA receptor blockers [11]. Over-stimulation of NMDA receptors expressed in differentiated P19 cells leads to death, which can be blocked with the specific NMDA channel blocker MK-801 [11]. These reports reveal that differentiated P19 cells recapitulate some important properties of glutamate excitotoxicity, and thereby appear to be an excellent model system for investigating NMDA receptor-dependent excitotoxic-signaling pathways.

In this study, we report that a selective inhibitor of MEK1/2, the ERK1/2 (p44/42) MAP kinase upstream activating enzymes [15], prevents glutamate-induced differentiated P19 cell death when added before or hours after glutamate challenge. This compound, 1,4-diamino-2,3-dicyano-1,4-bis[2-aminophenylthio]butadiene (U0126), blocked glutamate-induced increases in ERK2 (p42) MAP kinase phosphorylation in differentiated P19 cells. Glutamate-induced toxicity and intracellular calcium responses were blocked completely by MK-801, indicating that NMDA receptor activation is required for glutamate-induced toxic signaling in these cells. U0126 had no effect on glutamate-induced intracellular calcium responses, or NMDA receptor binding, indicating that its mechanism of protection is downstream of NMDA receptor activation.

2. Materials and methods

2.1. Materials

Fluorescent indicator dyes were obtained from Molecular Probes unless indicated otherwise. U0126 and various other commercially available protein kinase inhibitors were obtained from Calbiochem. MK-801 was obtained from Research Biochemicals Inc. Anti-p44/42 MAP kinase and anti-phospho-p44/42 MAP kinase antibodies were obtained from New England BioLabs. Polyclonal antibodies to rat NMDA receptor subunits NR1, NR2A, and NR2B were obtained from Chemicon. 6-Amino-2-(4-fluorophenyl)-4-methoxy-3-(4-pyridyl)-1*H*-pyrrolo-[2,3-*b*]pyridine (RWJ 68354) was synthesized at the R.W. Johnson Pharmaceutical Research Institute and was described previously [16].

2.2. P19 cell differentiation

P19 cells were bought from ATCC. They were grown on 150 cm^2 tissue culture flasks in Dulbecco's Modified Eagle's Medium (DMEM, Gibco BRL) supplemented with 10% fetal bovine serum, glutamine (2 mM), sodium pyruvate (1 mM), sodium bicarbonate (0.15%, w/v), and penicillin/streptomycin (50 U/mL) in an atmosphere of 5% CO_2 at 37°. On day 1 of the differentiation protocol, confluent P19 cells were split to 50–70% confluency in growth medium. On day 2 of the protocol, 10 μM ATRA and 10 μM MK-801 were added to the growth medium. Ten micromolar MK-801 was included at this stage to prevent the death of differentiating cells that begin to express NMDA receptors. On day 4, fresh growth medium was placed on the cells, with fresh ATRA and MK-801. On day 5, cells were dissociated from the tissue culture flask by washing four times with calcium- and magnesium-free phosphate-buffered saline, and adding 4 mL of non-enzymatic cell dissociation solution (Sigma). Once dissociated, cells were

placed in 40 mL of differentiation medium. Differentiation medium consisted of Neurobasal medium (Gibco BRL) containing 1% N-2 supplement (Gibco BRL), 0.1% trace elements B (Mediatech), 1 mM cadmium sulfate (Sigma), 2 mM glutamine, 1 mM sodium pyruvate, 0.15% (w/v) sodium bicarbonate, and 1% antibiotic/antimycotic (Gibco BRL). Ten micromolar cytosine-d-arabinofuranoside was added to the differentiation medium to prevent the growth of undifferentiated cells. No MK-801 was present from this point onward. Cells were triturated twenty times, then were split 1:4 into 96-well plates, or split 1:3 into 100 mm tissue culture dishes. Four days after replating, the cells were at an optimal stage for compound addition, and were assayed 24 hr later.

2.3. RT-PCR

Total RNA was extracted from differentiated P19 neurons or undifferentiated P19 cells in 100 mm tissue culture dishes using the QIAGEN RNeasy Mini kit according to protocols of the manufacturer. Real time RT–PCR reactions were carried out in LightCycler™ glass capillaries using a LightCycler™ instrument with 250 ng of template RNA (Boehringer Mannheim). The reverse transcriptase reaction was carried out for 10 min at 55°. PCR was carried out for 30 cycles: annealing temperature was 50°, extension temperature was 72°, and melting temperature was 80°. Reactions were compared to an H_2O negative control for each primer set. Products were analyzed on both 1% Tris-borate-EDTA (TBE)-buffered-agarose gels and the LightCycler™. The primer sets for the various mouse NMDA receptor subunits that were used are as follows: zeta1 5′ primer: 5′-gaa gat aca gct caa cgc ca-3′; zeta1 3′ primer: 5′-tcc tcg ctt gca gaa agg at-3′; epsilon1 5′ primer: 5′-cgg cag ctt tgg aag aaa tc-3′; epsilon1 3′ primer: 5′-cag aca ggc atc aca ctt ga-3′; epsilon2 5′ primer: 5′-aga cca caa gcg cta ctt ca-3′; epsilon2 3′ primer: 5′-cgt gaa gca agc act gat ca; epsilon 3 5′ primer: 5′-gcc aat gtg ctg aag atg ct-3′; epsilon3 3′ primer: 5′-ttg gat cga gtg aag gct tc-3′; epsilon4 5′ primer: 5′-gtg tct tct aca tgc tcc tc-3′; and epsilon4 3′ primer: 5′-agc ttg tca acc gac cag ta-3′.

2.4. Western blots

Medium was aspirated from cells plated onto 100 mm tissue culture dishes. Cells were harvested in RIPA lysis buffer [100 mM Tris–HCl (pH 7.5), 150 mM NaCl, 1 mM EDTA, 1% Triton X-100, 10% sodium deoxycholate, 0.1% sodium dodecyl sulfate]. Each sample was sonicated for 20 sec, Laemmli sample buffer (BioRad) was added to a final 1x concentration, and samples were incubated for 10 min at 95°. Samples to be probed with NMDA receptor antibodies were electrophoresed on 6% Tris-glycine pre-cast gels (Novex). Samples to be probed with p44/42 MAP kinase antibodies were electrophoresed on 12% Tris-glycine pre-cast gels (Novex). Electrophoresis was carried out in a Novex apparatus for 1.5 hr at 200 V. Proteins were transferred to polyvinylidene difluoride membranes (PVDF, Novex) using a BioRad wet transfer device for 1 hr at 100 V. Prior to transfer, PVDF membranes were dipped in 100% methanol for 1 min, and then were soaked in transfer buffer for 5 min. After transfer, membranes were removed and were shaken slowly in blocking solution (5% milk, 0.05% Tween-20 in phosphate-buffered saline) at 4° overnight. Membranes were then washed once with PBS-Tween, and primary antibodies (1:1000) in PBS-Tween with 5% milk were incubated for 1 hr at room temperature. Membranes were washed four times for 15 min at room temperature. Secondary antibodies coupled to horseradish peroxidase were incubated for 45 min to 1 hr at room temperature in PBS-Tween with 5% milk. Membranes were then washed four times for 15 min at room temperature. Blots were developed using ECL Plus (Amersham), and exposed to film.

2.5. Cytotoxicity measurements

Cell viability was measured using two methods. The first method was a confocal, single-cell fluorescence imaging based method using the live cell dye CFDA. CFDA is de-acetylated, and is thus trapped and concentrated inside live cells. Hence, CFDA selectively labels the cell bodies and processes of living cells, whereas dead cells exhibit much less CFDA staining. Cells were labeled with 1 μM CFDA for 15 min in medium, and then CFDA staining was imaged using a modified Attofluor® Imager device (Atto Instruments). The dye was excited by light from a mercury lamp source passed through a 488 nm bandpass filter of 10 nm band width, passed through a CARV real-time confocal spinning disk module (Atto Instruments), and then passed through a 40x oil immersion objective (Zeiss Fluar, NA=1.3). Emitted light was transmitted through a 495 nm dichroic mirror, collected to an Attofluor® intensified CCD camera, and images were visualized using Attofluor® RatioVision® software (Atto Instruments).

The second method for measuring cell viability was a plate reader method. Cells plated into black 96-well plates (Packard Viewplates) were loaded with a final concentration of 3% Alamar blue dye (Biosource International). Alamar blue is a dye that takes advantage of mitochondrial reductases to convert non-fluorescent resazurin to fluorescent resorufin (excitation 535 nm, emission 580 nm). This dye has been used successfully to measure neuronal viability in primary neuronal culture [17]. Baseline fluorescence counts were read at room temperature in a Wallac plate reader immediately after the addition of Alamar blue. Fluorescence counts of cell viability were taken the same way after a 1-hr incubation at 37°. Fluorescence was expressed as a percent of control, untreated cells, after subtraction of background fluorescence. Live/dead cells were confirmed visually with a light microscope.

Table 1
Substrates and control inhibitors for kinase selectivity assays

Kinase	Substrate name	Peptide sequence	Control inhibitor
CDK1	Histone-H_1	(Biotin)KTPKKAKKPKTPKKAKKL-Amide	Butyrolactone
EGFR	Angiotensin 2	(Biotin)DRVYIHPF-Amide	AG-1478
PKA	BetterThanKemptide	(Biotin)GRTGRRNSI-Amide	H-89
PKC	PKC pseudopeptide	(Biotin)RFARKGSLRQKNV-NH_2	Staurosporine
Casein kinase 1	Glycogen synthase	(Biotin)KRRRALS(phospho)VASLPGL-Amide	H-89
Casein kinase 2	Nef	(Biotin)RREEETEEE-Amide	
Calmodulin kinase	AutoCamtide II	(Biotin)KKALRRQETVDAL-Amide	Staurosporine
Insulin kinase	Kinase domain	(Biotin)TRDIYETDYYRK-Amide	Staurosporine

2.6. Fura-2 imaging

Cells were loaded with 5 μM fura-2-AM (Molecular Probes) for 1 hr at 37°. They were washed once with Hanks' balanced salt solution (HBSS, Gibco BRL), and assayed in HBSS buffer. Cells were placed onto the stage of a modified Attofluor® Imager. High speed, dual excitation of fura-2 was carried out using a RatioArc High-Speed Excitor, which rapidly switches excitation light between 334 and 380 nm wavelengths (10 nm band width filters). Emitted light was transmitted through a 400-nm dichroic mirror, collected to an Attofluor® intensified CCD camera, and ratio-images were visualized, and analyzed, using Attofluor® RatioVision® software.

2.7. [^{3}H]MK-801 binding

Cell membranes were prepared by freeze–thawing 100 mm plates of cells; then the contents of the plates were transferred to 15-mL centrifuge tubes. The cells were spun at 50,000 *g* for 20 min at 4°. The pellets were then suspended in a membrane wash solution containing 100 μM glutamate, 100 μM glycine, 100 μM $MgCl_2$, and 50 mM Tris to remove any unbound MK-801. The suspensions were spun and resuspended in wash solution a total of three times. The final membrane pellets were resuspended in 20 mM HEPES, 100 μM glutamate, 100 μM glycine, 300 μM $MgCl_2$, and 100 μM spermine to facilitate ligand binding (pH 7.4). The membrane suspensions were pipetted into 96-well plates. Each well contained 20 nM [^{3}H]MK-801, 100 μL of cell membranes, and various concentrations of MK-801. Nonspecific binding was defined as [^{3}H]MK-801 binding in the presence of 10 μM unlabeled MK-801. The final assay volume was 150 μL. Plates were then incubated at 37° for 3 hr. After incubation, cell membranes were vacuum-filtered onto Packard unifilter plates, using a Packard filtration manifold, and the membranes were washed three times with ice-cold 20 mM HEPES. Filters were then sealed, 35 μL of Packard Microscint 20 scintillation fluid was added per well, and the filters were covered with a cellophane seal over the top. Plates were then counted for 1 min/well in a Packard Topcount. Displacement of MK-801 binding was expressed as percent of control.

2.8. In vitro kinase assays

The general procedure used to assay for kinase activity was as follows: a kinase reaction mix was prepared in 50 mM Tris–HCl (pH 8), 10 mM $MgCl_2$, 0.1 mM Na_3VO_4, 1 mM dithiothreitol, 10 μM ATP, 0.25 to 1 μM biotinylated peptide substrate, 0.2 to 0.8 μCi per well of [γ-^{33}P]ATP (2000–3000 Ci/mmol). The reaction mix was dispensed into the wells of a streptavidin-coated Flashplate (New England Nuclear), and 1 μL of inhibitor stock in 100% DMSO was added to a 100-μL reaction volume resulting in a final concentration of 1% DMSO. Enzyme was diluted in 50 mM Tris–HCl (pH 8.0), 0.1% BSA and added to each well. The reaction was incubated for 1 hr at 30° in the presence of compound. After 1 hr, the reaction mix was aspirated from the plate and the plate was washed with PBS containing 100 mM EDTA. The plate was read in a scintillation counter to determine the amount of [γ-^{33}P]ATP incorporated into the immobilized peptide. Test compounds were assayed in duplicate at eight concentrations ranging from 100 μM to 10 pM in one order of magnitude steps. A maximum signal and a minimum signal for the assay were determined on each plate. The IC_{50} value was calculated from the concentration–response curve of the percent inhibition of the maximum signal in the assay according to the formula [max signal −background/test compound signal - background [100] = % inhibition] by graphing the percent inhibition against the log concentration of the test compound. Known inhibitor compounds appropriate for the kinases being assayed were also included on each plate (see Table 1 for kinase substrates and control inhibitors). The human CDK1 catalytic subunit and its positive regulatory subunit cyclin B were expressed recombinantly from insect cells using a baculovirus vector (New England BioLabs). Insulin receptor kinase consisted of residues 941-1313 of the cytoplasmic domain of the beta-subunit of the human insulin receptor (BIOMOL). PKA was the catalytic subunit of cyclic AMP-dependent PKA purified from bovine heart (Upstate Biotechnology). PKC was the gamma isoform of the human protein produced in insect cells (PanVera). Casein kinase 1 was a truncation at amino acid 318 of the C-terminal portion of the rat CK1 delta isoform produced in *Escherichia coli* (New England BioLabs). Casein kinase 2

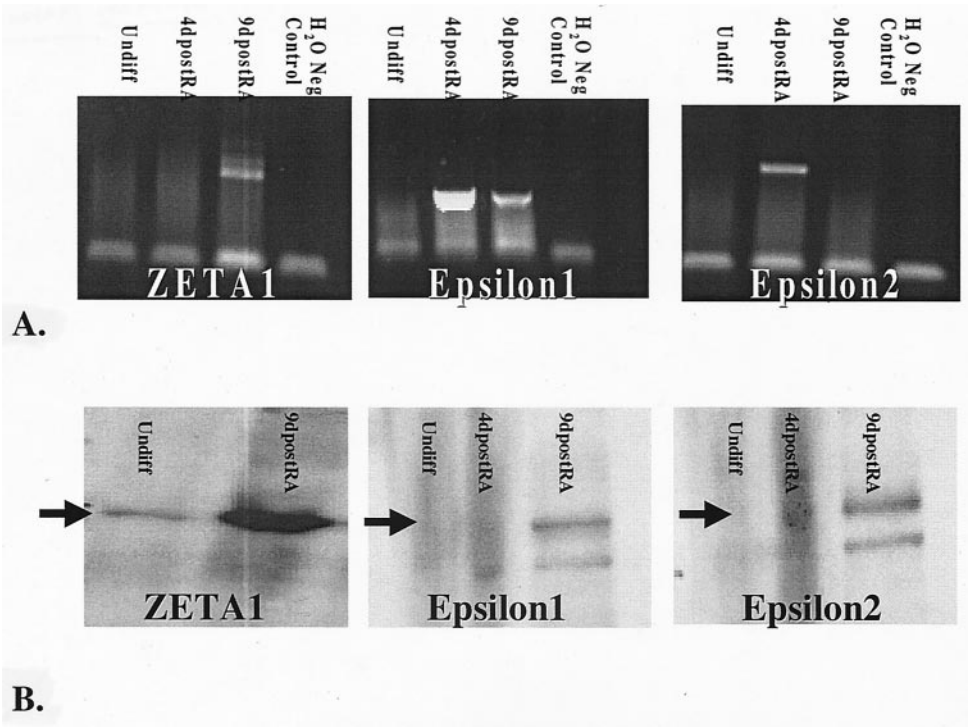

Fig. 1. NMDA receptor expression in differentiating P19 cells. (A) RT–PCR amplification of murine NMDA receptor subunits was obtained from 250 ng of total RNA template isolated from undifferentiated P19 cells, cells at 4 days after induction by ATRA, and cells at 9 days after ATRA induction. RT–PCR was carried out in a LightCycler™ instrument as described in "Materials and methods." For each primer set, an H_2O negative control was run in parallel to ensure that products were not the result of primer-dimer. Five microliters of reaction product was removed, and run on 1x TBE agarose gels. These data are representative of three separate experiments with similar results. (B) Western blot analysis of NMDA receptor subunit protein in P19 cell lysates harvested at various time points during the course of differentiation. Appropriately sized bands (zeta1 = ~120 kDa, epsilon1 and epsilon 2 = ~180 kDa) were detectable from terminally differentiated P19 cell lysates, but not from undifferentiated cell lysates. Black arrows indicate which bands correspond to the NMDA receptor subunits. These data are representative of three separate experiments with similar results. (C) Fura-2 imaging traces of 9-day post ATRA P19 cells treated with 3 mM glutamate and 1 mM glycine in the presence or absence of 100 μM MK-801. MK-801 was administered 24 hr prior to the assay. Traces represent the means ± SEM from three separate experiments for each condition. Each experiment represents the average ratio change from 10–20 cells, equivalent to the total number of cells in the microscopic field. (D) MK-801 inhibition of [^{3}H]MK-801 specific binding in differentiated P19 cell membranes harvested 9 days after ATRA induction. MK-801 concentrations are expressed as 10^{-x} molar. Data points represent the means ± SEM from eight experiments. % Control = $[(cpm - cpm_{min})/(cpm_{max} - cpm_{min})] \cdot 100$.

included the alpha and beta subunits of the human CK2 protein produced in *E. coli* (New England BioLabs). Calmodulin kinase (calmodulin-dependent protein kinase 2) was a truncated version of the alpha subunit of the rat protein produced in insect cells (New England BioLabs). EGFR was purified from human A431 cell membranes (Sigma).

3. Results

3.1. Expression of functional NMDA receptors in differentiated P19 cells

P19 cells were differentiated for 4 days in the presence of retinoic acid, and then were replated onto 100 mm tissue culture plates for 5 additional days in the presence of cytosine arabinoside, a mitotic inhibitor. At this time, virtually all the cells appeared morphologically very similar to mature primary neurons; however, exact quantification of the proportion of precursor P19 cells that became neurons was not determined. Cells were harvested for mRNA analysis and protein analysis at 4 or 9 days after induction by retinoic acid. RT–PCR of NMDA receptor subunits from total RNA samples revealed that retinoic acid induction of differentiation induced mRNA expression of zeta1, epsilon1, and epsilon2 mRNAs (Fig. 1A). Western blot analysis revealed that terminally differentiated P19 cells express detectable levels of zeta1, epsilon1, and epsilon 2 proteins (Fig. 1B). Epsilon3 and epsilon4 mRNAs or proteins were not detectable at any time in these cells (data not shown). To verify that differentiated P19 cells express specific binding sites for the NMDA receptor, MK-801 inhibition of [^{3}H]MK-801 binding was assayed in P19 membranes (Fig. 1D). MK-801 inhibition was concentration dependent, and 100% inhibition was achieved.

To determine whether the expressed NMDA receptor subunits form functional NMDA receptors, intracellular calcium measurements were carried out in differentiated P19 cells. Single cell fura-2 imaging experiments revealed in-

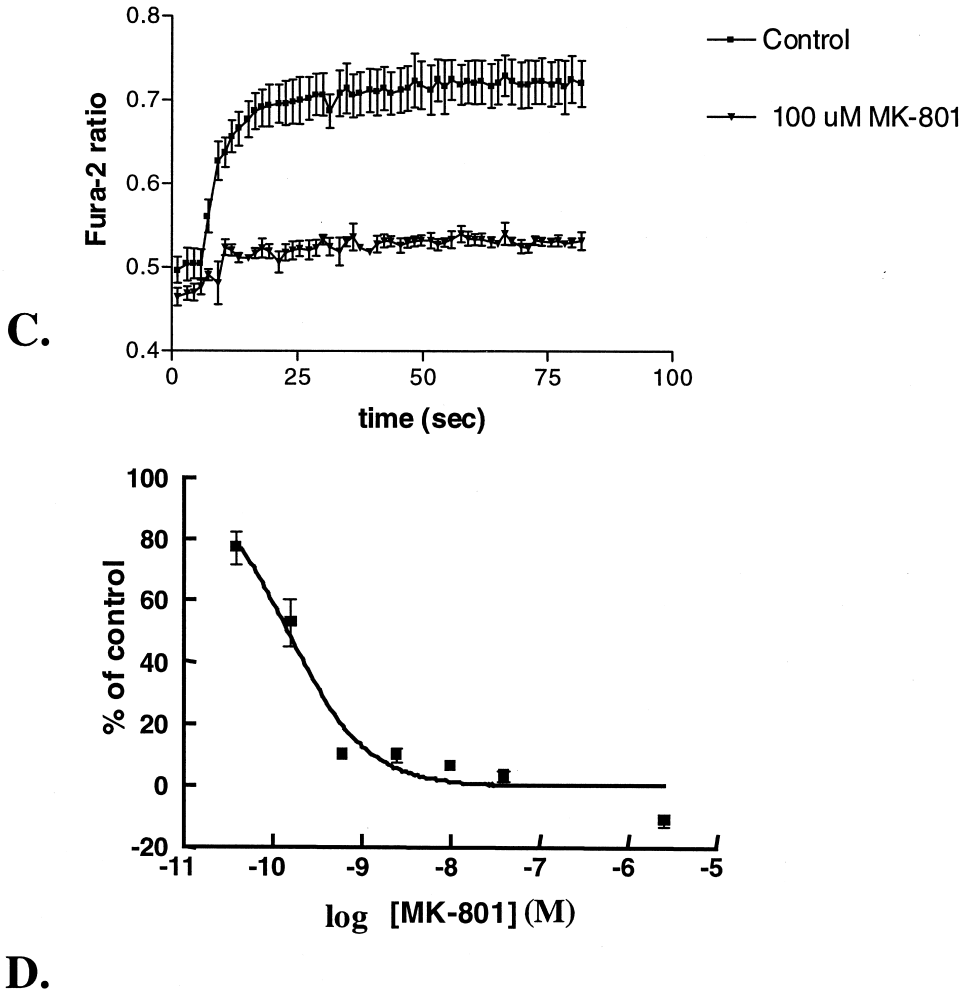

Fig. 1. *(continued)*

creases in intracellular calcium levels upon the addition of glutamate and the NMDA receptor requisite coagonist glycine (Fig. 1C). The rise in intracellular calcium level was rapid, occurring within 10–20 sec, and was sustained for minutes afterward. Although glutamate, in principle, could activate other classes of glutamate receptors that may be expressed in differentiated P19 cells, the calcium response to glutamate that we observed requires NMDA receptor activation, since the selective NMDA receptor channel blocker, MK-801, nearly completely inhibited this response (Fig. 1C).

3.2. NMDA receptor-required toxicity in differentiated P19 cells

Differentiated P19 cell bodies and processes stained brightly with the vital cell stain CFDA (Fig. 2A). The cell bodies characteristically clumped together into tight aggregates when plated onto plain tissue culture plastic, prohibiting visualization of individual cell bodies. Visually detectable networks of extensive processes connected clusters of cell bodies. Differentiated P19 cells treated with saturating concentrations of glutamate and glycine (3 and 1 mM, respectively) for 24 hr exhibited much weaker overall fluorescence staining, suggesting lower viability in these treated cells. Processes were undetectable, and extensive cellular debris was evident (Fig. 2A). Relative levels of cell death can be measured rapidly and quantitatively on a plate reader using Alamar blue, a dye previously shown to be useful for assessment of neuronal viability [17] (Fig. 2B). Background fluorescence, read immediately after dye addition, was subtracted from fluorescence derived from active mitochondrial reduction of Alamar blue to its more fluorescent derivative, resorufin, which was read at 1 hr after 37° incubation. The data were measured in the form of relative fluorescence counts (Fig. 2B). Healthy differentiated P19 cells effectively converted Alamar blue to fluorescent resorufin, and increased the fluorescence counts by over 100,000 arbitrary fluorescence units (AFU). Cells treated with glutamate and glycine for 24 hr largely lost the ability to reduce Alamar blue, and hence only increased fluorescence by approximately 40,000 AFU, corresponding to a

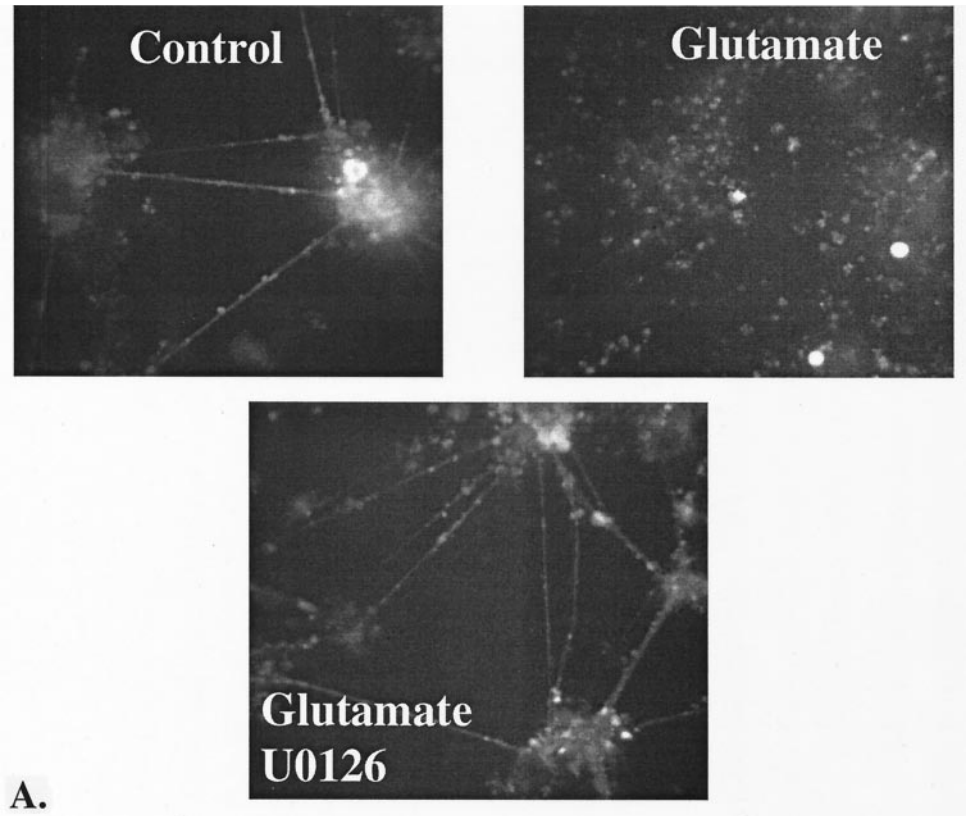

Fig. 2. NMDA receptor-required glutamate toxicity in differentiated P19 cells. (A) At 9 days post ATRA induction, P19 cells were labeled with CFDA, and then imaged in confocal mode using an Attofluor® Imager as described in "Materials and methods." Control cells were treated with vehicle for 24 hr, glutamate cells received 3 mM glutamate in the presence of 1 mM glycine for 24 hr, and glutamate + U0126 cells received 10 μM U0126 concurrent with 3 mM glutamate and 1 mM glycine for 24 hr. Images are representative of three separate experiments per condition with similar results. (B) Representative raw data from a single 96-well plate where values are the mean Alamar blue fluorescence counts ± SEM in which 32 wells received vehicle control, 32 wells received 3 mM glutamate and 1 mM glycine for 24 hr, and 32 wells received 5 μM A23187 for 24 hr. Glutamate and A23187 conditions were significantly different from control as determined by one-way ANOVA with Tukey post-hoc analysis carried out using GraphPad software (***$P < 0.001$). These raw data indicate a typical 60% reduction in Alamar blue fluorescence when cells were treated with glutamate and glycine. However, since raw fluorescence counts varied from experiment to experiment, all the following figures are expressed as a percent of control. (C) Glutamate toxicity concentration–response in the presence of a constant 1 mM glycine concentration. The theoretical curve generated through the data points is the average of six separate concentration–response curves. Data points are represented as percent of control cells ± SEM. % Control = (([Glutamate]$_{exp}$ – [Glutamate]$_{max}$)/(Control$_{vehicle}$ – [Glutamate]$_{max}$)) · 100. Glutamate toxicity EC_{50} was calculated to be 8.1 μM [lower 95% confidence interval = 3.5 μM; upper 95% confidence interval = 19 μM]. (D) MK-801 concentration-dependent inhibition of differentiated P19 cell death induced by 3 mM glutamate and 1 mM glycine. % Neuroprotection = ((Inhibitor in the presence of Glutamate$_{max}$ – [Glutamate]$_{max}$)/(Control$_{vehicle}$ – [Glutamate]$_{max}$)) · 100. Data points are the means ± SEM of three separate experiments. Key: (**) $P < 0.01$, and (***) $P < 0.001$ versus the lowest concentration of MK-801.

60% reduction in the ability to reduce Alamar blue. As a control, a calcium ionophore, A23187, which is also very toxic to differentiated P19 cells, caused these cells to nearly lose the ability to reduce Alamar blue. Glycine, in the absence of glutamate, did not affect P19 neuron viability. Yet, in the presence of glutamate, glycine enhanced the reproducibility of glutamate-induced differentiated P19 cell death (data not shown). This glycine requirement is consistent with classical NMDA receptor pharmacology [18].

We used the Alamar blue assay to quantify the concentration effect of the glutamate-induced loss in differentiated P19 cell viability (Fig. 2C). Very little effect on cell viability was evident until glutamate reached micromolar concentrations. Consistent with morphological observations, glutamate toxicity was maximal at greater than 100 μM concentrations. The EC_{50} value for glutamate toxicity in differentiated P19 cells was 8.1 μM. The NMDA receptor blocker, MK-801, concentration-dependently protected against glutamate toxicity (Fig. 2D). At 30 and 100 μM, MK-801 nearly completely blocked glutamate toxicity.

3.3. Protection from glutamate toxicity by an inhibitor of MEK1/2 in differentiated P19 cells

To evaluate the specificity of the protein kinase pathways involved in differentiated P19 cell glutamate toxicity, a panel of various classes of protein kinase inhibitors were tested (Table 2). To consistently induce the maximal amount of cell death, and to set a rigorous screen for the inhibitors of this process, we chose saturating concentrations of glutamate (3 mM) and glycine (1 mM) throughout the studies. While inhibitors of PKA, PKC, and protein

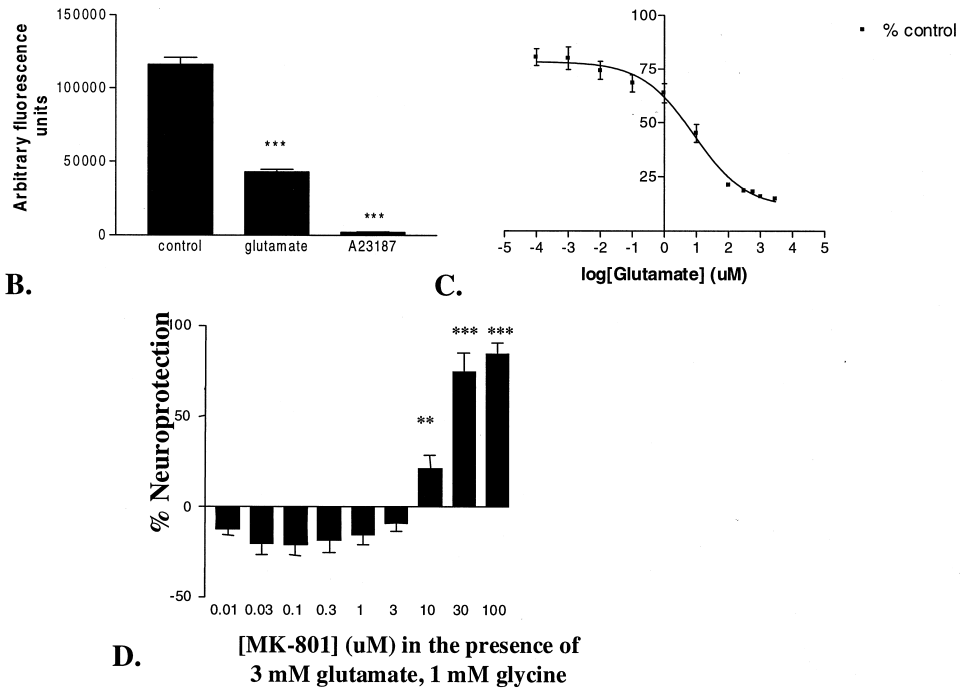

Fig. 2. *(continued)*

tyrosine kinases [19–24] were not very protective, two MAP kinase inhibitors, RWJ 68354 and U0126, achieved maximal protection against glutamate-induced cell death. RWJ 68354, a very potent p38 kinase inhibitor, exhibited a 1000-fold lower potency for protection against cell death (IC_{50} of 9.7 μM) than for *in vitro* p38 enzyme inhibition (IC_{50} of ~10 nM) (Table 2, Fig. 3). Other potent p38 kinase inhibitors of various structural classes were not protective, suggesting that p38 kinase inhibition is likely not a predominant mechanism of protection against glutamate toxicity in these cells. A second protective compound that was identified, U0126, exhibited an IC_{50} of 1.1 μM, which more closely matches the IC_{50} that has been reported for inhibition of wild-type MEK1/2 enzymes *in vitro* [15] (Table 2, Figs. 2A and 3B). The maximal protection achieved by U0126 was greater than 80% of the vehicle-treated controls.

Table 2
Comparison of kinase inhibitor activity to cytoprotective activity

Compound ID	Enzyme target	Activity	Potency	IC_{50} for cytoprotection [lower–upper 95% C.I.]	Maximal efficacy for cytoprotection, (%)
RWJ 68354	p38 kinase	Inhibitor	IC_{50} ~10 nM	9.7 μM [5.8–16.3]	>80
U0126	MEK 1/2	Inhibitor	IC_{50} ~0.5 μM	1.1 μM [0.74–1.68]	>80
SB202474	p38 kinase	Inactive	Nonapplicable	>10 μ M	>50
SB203580	p38 kinase	Inhibitor	IC_{50} ~600 nM	Ineffective	<10
Lithium	IP_3 turnover	Inhibitor	K_i ~0.5 μM	Ineffective	<10
KN62	CAM-KII	Inhibitor	K_i ~900 nM	Ineffective	<10
Calphostin C	PKC	Inhibitor	IC_{50} ~50 μM	>1 μM	~50
	PKA	Inhibitor	IC_{50} >50 μM		
	PKG	Inhibitor	IC_{50} >25 μM		
	$p60^{c\text{-}src}$	Inhibitor	IC_{50} >50 μM		
Lavendustin A	EGFR	Inhibitor	IC_{50} ~11 nM	>10 μM	<25
	$p60^{c\text{-}src}$	Inhibitor	IC_{50} ~500 nM		
H-89	PKA	Inhibitor	K_i ~48 nM	>10 μM	<2
	CAM-KII	Inhibitor	K_i ~30 μM		
	Casein kinase I	Inhibitor	K_i ~38 μM		
	PKC	Inhibitor	K_i ~31.7 μM		

Kinase inhibition activities and potencies were derived from the literature [15,16,19–24]. Each IC_{50} value for cytoprotection is the mean of three separate curves with upper and lower 95% confidence intervals (C.I.) shown. Curves were fit, and confidence intervals were determined using GraphPad Prism software.

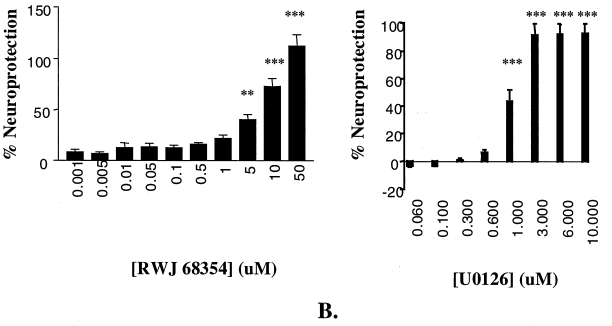

Fig. 3. Kinase inhibitor protection against glutamate toxicity in differentiated P19 cells. (A) RWJ 68354 concentration-dependent inhibition of P19 cell death induced by 3 mM glutamate and 1 mM glycine. % Neuroprotection = ((Inhibitor in the presence of $Glutamate_{max}$ – $[Glutamate]_{max}$)/($Control_{vehicle}$ – $[Glutamate]_{max}$)) 100. Data points are the means ± SEM of three separate experiments. Key: (**) $P < 0.01$, and (***) $P < 0.001$ versus the lowest concentration of RWJ 68354. The EC_{50} value for inhibition of toxicity was calculated to be 9.7 μM (5.8 to 16.3 μM). (B) U0126 concentration-dependent inhibition of P19 cell death induced by 3 mM glutamate and 1 mM glycine. % Neuroprotection is the same as described for panel A. Data points are the means ± SEM of three experiments. Key: (***) $P < 0.001$ versus the lowest concentration of U0126. The EC_{50} value for inhibition of toxicity was calculated to be 1.1 μM (0.74 to 1.68 μM).

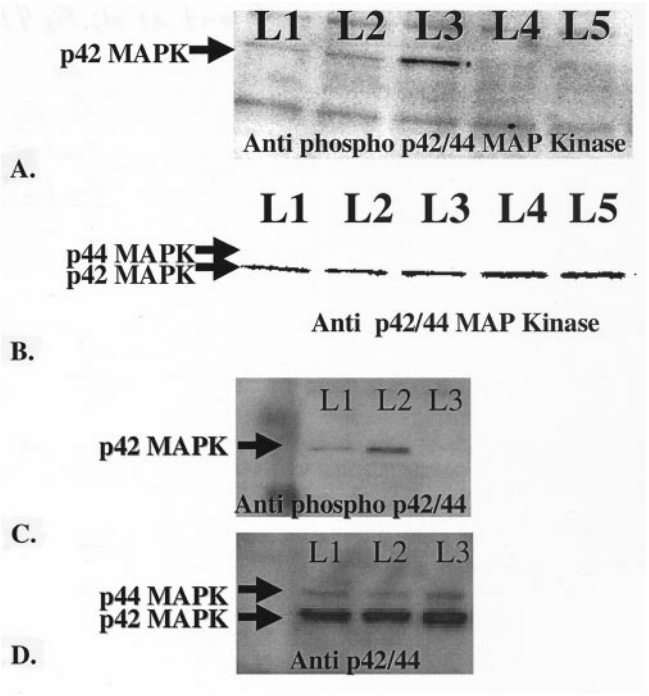

Fig. 4. p44/42 MAP kinase phosphorylation in differentiated P19 cells and inhibition with U0126. (A) Western blot probing 9-day post ATRA P19 cell lysates with an antibody specific for the phosphorylated form of p42/44 (ERK1/2). L1 = 5-min vehicle control; L2 = 1 min, 3 mM glutamate, 1 mM glycine; L3 = 5 min, 3 mM glutamate, 1 mM glycine; L4 = 1 min, 3 mM glutamate, 1 mM glycine with concurrent 10 μM U0126; and L5 = 5 min, 3 mM glutamate, 1 mM glycine with concurrent 10 μM U0126. (B) Same blot as in panel A, but stripped and reprobed with an antibody that recognizes total p42/44 (ERK1/2). (C) Anti-phospho p42/44 (ERK1/2) antibody western blot of differentiated P19 cell lysates at a 24-hr time point. L1 = 24-hr vehicle control; L2 = 24 hr, 3 mM glutamate, 1 mM glycine; L3 = 24 hr, 3 mM glutamate, 1 mM glycine with concurrent 10 μM U0126. (D) Same blot as in panel C, but stripped and reprobed with an antibody that recognizes total p42/44 (ERK1/2). These blots are representative of three separate experiments with similar results.

Although U0126 is reported to be highly selective for MEK1/2 [15], we generated specificity data against a panel of kinase enzymes to determine whether MEK1/2 inhibition is a likely protective mechanism, or whether inhibition of other kinase enzymes could be involved (Table 3). RWJ 68354 was run in parallel to assess whether this compound shared any common properties with U0126 (Table 3). Consistent with what has been published previously [15], U0126 was not active against many other kinase enzymes. One other kinase which we found to be inhibited by U0126 is PKC-γ. However, its IC_{50} for inhibition of this enzyme was 29.5 μM, 30-fold higher than its protective potency, and 60-fold higher than its published IC_{50} against wild-type MEK1/2. RWJ 68354 was a somewhat less selective inhibitor. In addition to its known high potency inhibition of p38 [16], this compound also inhibited casein kinase-1 with an IC_{50} value of 0.116 μM, and inhibited PKC-γ with lower potency (Table 3).

To determine whether U0126 inhibits the MEK1/2 enzymes in differentiated P19 cells, we tested its ability to block glutamate-induced phosphorylation of the MEK1/2 substrate p44/42 MAP kinase (ERK1/2). The data demonstrated that the concentrations of glutamate and glycine that were used to induce toxicity in P19 neurons also induced a rapid, reproducible increase in p42 (ERK2) MAP kinase phosphorylation in these cells (Fig. 4A). In the presence of U0126, phospho-p42 MAP kinase was reduced, although no change in the amount of total p42 MAP kinase was evident (Fig. 4, A and B). In glutamate-treated cells, the elevation of p42 MAP kinase phosphorylation was sustained, since it was still clearly increased at 24 hr versus controls (Fig. 4C). U0126 blocked the increased levels of phosphorylation at

Table 3
Kinase selectivity of RWJ 68354 and U0126

Compound	CDK1 (μM)	EGFR (μM)	PKA (μM)	PKC-γ (μM)	Casein kinase 1 (μM)	Casein kinase 2 (μM)	Calmodulin kinase (μM)	Insulin receptor kinase (μM)
RWJ 68354	>100	>100	>100	8.35	0.116	>100	>100	>100
U0126	>100	>100	>100	29.5	>100	>100	>100	ND

Each IC_{50} value for kinase inhibition is the mean of at least two separate curves, and was determined using GraphPad curve fitting software. ND = not determined.

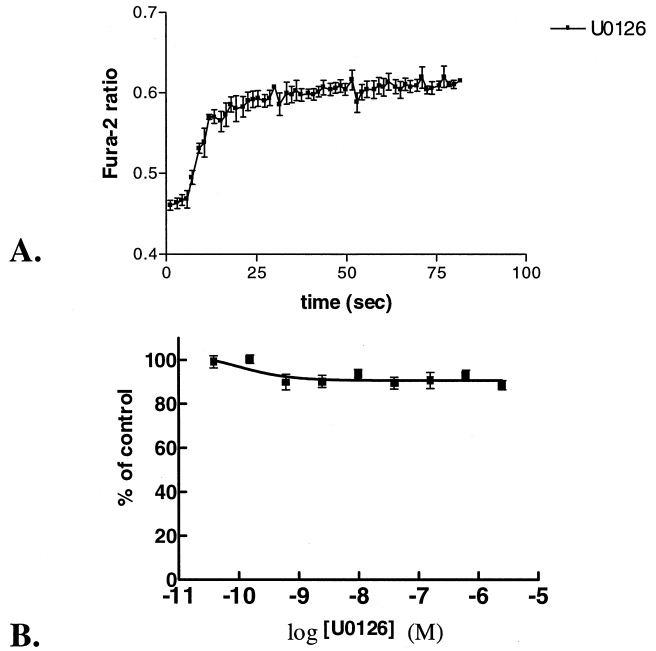

Fig. 5. Lack of U0126 block of NMDA receptor activation. (A) Fura-2 imaging traces of 9-day post ATRA P19 neurons treated with 3 mM glutamate, 1 mM glycine in the presence of 10 μM U0126 for 24 hr. U0126 was administered concurrently with glutamate and glycine. Traces represent the means ± SEM from four separate experiments for each condition. Each experiment represents the average ratio change from 10–20 cells, equivalent to the total number of cells in the microscopic field. (B) U0126 inhibition of [^{3}H]MK-801 specific binding in differentiated P19 cell membranes harvested 9 days after induction by ATRA. Data points represent the means ± SEM from eight experiments. % Control is defined as described in the legend to Fig. 1D.

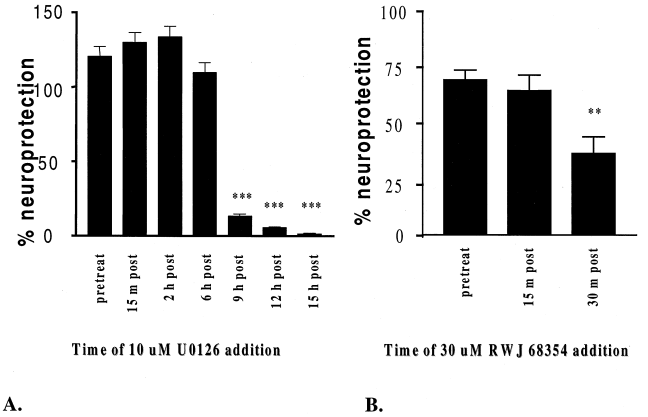

A. B.

Fig. 6. Maximal protective efficacy of U0126, but not of RWJ 68354, upon administration hours after onset of glutamate challenge. (A) Differentiated P19 cells received 10 μM U0126 either 15 min prior to glutamate and glycine addition, or 15 min, 2 hr, 6 hr, 9 hr, 12 hr, or 15 hr after the addition of glutamate and glycine. Twenty-four hours later, cells were assayed for Alamar blue fluorescence. Data are the means ± SEM from eight separate experiments. Key: (***) $P < 0.001$ versus pretreatment control, determined by one-way ANOVA followed by Tukey post-hoc analysis. (B) Differentiated P19 cells received 30 μM RWJ 68354 15 min prior to glutamate and glycine addition, or 15 min or 30 min after the addition of glutamate and glycine. Twenty-four hours later, cells were assayed for Alamar blue fluorescence. Data are the means ± SEM from three separate experiments. Key: (**) $P < 0.01$ versus pretreatment control determined by one-way ANOVA followed by Tukey post-hoc analysis.

this time point as well (Fig. 4C) without affecting the level of total p42 MAP kinase (Fig. 4D).

To demonstrate that U0126 does not block the NMDA receptor directly, but rather intervenes at a downstream signaling event, we tested differentiated P19 cell intracellular calcium responses to glutamate and glycine in the presence of 10 μM U0126 (Fig. 5A). Unlike MK-801, which completely blocks NMDA receptor activation and calcium influx, U0126 did not block this intracellular calcium response. Additionally, we tested whether U0126 could inhibit [^{3}H]MK-801 specific binding in P19 neuron membranes (Fig. 5B). U0126 did not inhibit this binding activity at any concentration tested. These data further support the model that U0126 is acting on a signaling pathway downstream of glutamate signal transduction and NMDA receptor activation.

3.4. Delayed neuroprotection by the MEK inhibitor U0126

A time-course of efficacy is an extremely relevant parameter for a potential cytoprotective therapeutic agent, since the therapeutic would need to be administered hours to days after an ischemic event and still retain efficacy. We examined whether the MEK1/2 inhibitor U0126 retained cytoprotective efficacy when added at various time points after glutamate challenge. The data demonstrated that post-treatment with U0126 was just as protective to P19 neurons as pretreatment up to 6 hr after glutamate challenge (Fig. 6A). U0126 dramatically lost efficacy when added 9 hr or later after glutamate. In contrast, RWJ 68354, a known p38 inhibitor with an undetermined mechanism of cytoprotective action, lost efficacy as soon as 30 min after glutamate challenge (Fig. 6B).

3.5. Selectivity of U0126 protection against glutamate-induced toxicity

To determine whether U0126 is protective against a variety of nonspecific toxic insults, or whether the efficacy of this compound is selective for glutamate-induced toxicity, we tested its effects against a variety of other inducers of differentiated P19 cell death. The data demonstrated that U0126 is not protective against A23187- or staurosporine-induced death (Fig. 7, A and B). Additionally, U0126 did not affect the basal viability of differentiated P19 cells (Fig. 7C).

4. Discussion

The present study demonstrated that activation of the p44/42 MAP kinase pathway (ERK1/2) downstream of glu-

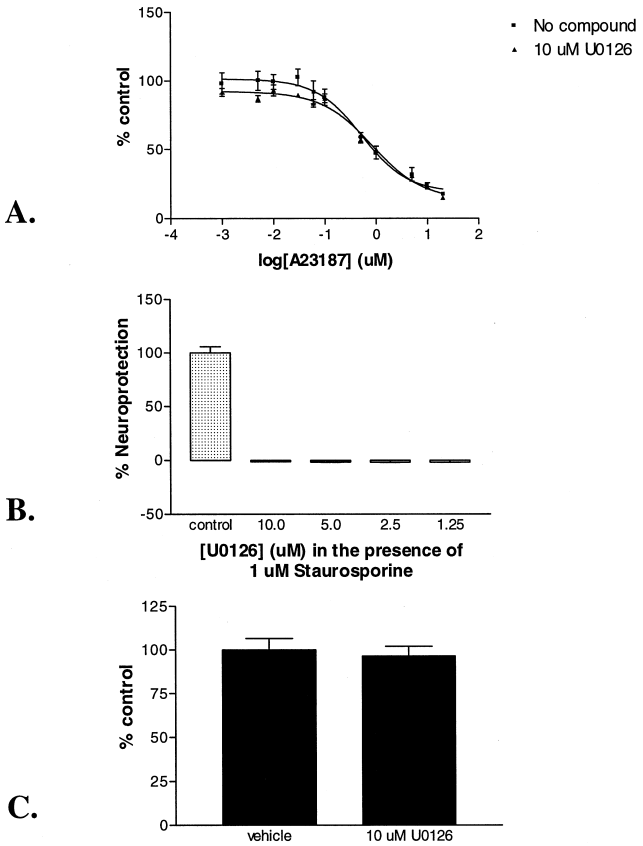

Fig. 7. Specificity of U0126 protection for glutamate toxicity in differentiated P19 cells. (A) P19 cells were treated with various concentrations of A23187 for 24 hr in the presence or absence of 10 μM U0126. Cells were then assayed for Alamar blue fluorescence. The theoretical curve generated through the data points is the average of three separate concentration–response curves. Data points are represented as percent of control cells ± SEM. The EC_{50} for A23187 toxicity in the absence of U0126 was calculated to be 520 nM (340 to 784 nM). The EC_{50} for A23187 toxicity in the presence of 10 μM U0126 was calculated to be 833 nM (440 nM to 1.6 μM). (B) Lack of 10 μM U0126 protection against differentiated P19 cell toxicity induced by 1 μM staurosporine measured by Alamar blue fluorescence at 24 hr after addition. Cells that received vehicle rather than staurosporine exhibited control levels of Alamar blue fluorescence. However, no concentration of U0126 brought fluorescence back to control levels in staurosporine-treated cells. Values are means ± SEM (N = 8). (C) Alamar blue fluorescence assayed on differentiated P19 cells treated with vehicle or with 10 μM U0126 in the absence of any inducers of toxicity. Values are the means ± SEM (N = 48).

tamate signal transduction is necessary for glutamate-induced toxicity in neuronally differentiated P19 cells. Glutamate-induced cell death occurred within 24 hr, was concentration-dependent, and required NMDA receptor activation. Glutamate induced phosphorylation of p42 MAP kinase, which was blocked by U0126, an inhibitor of its upstream kinase, MEK. U0126 also blocked glutamate toxicity in a concentration-dependent manner. It was effective when administered before, or even several hours after the onset of the glutamate challenge. In contrast, RWJ 68354, a p38 MAP kinase inhibitor with additional nonspecific activity at other kinases, exhibited some low potency cytoprotection upon pretreatment, but lost efficacy if added only minutes after the onset of glutamate challenge.

P19 neuron-like cells, derived from retinoic acid differentiation of murine teratocarcinoma cells, are a well-established clonal cell culture model of primary neurons [12,13] and are an appealing model system for neurobiology research and drug discovery. Unlike primary neurons, which are limited in amount and time-consuming to prepare, P19 precursor cells can be grown in large quantities, ideal for large-scale compound screens. P19 cells are also unlike neuroblastoma cell lines, which maintain proliferation capabilities but do not exhibit most terminally differentiated phenotypes. Differentiated P19 cells express a wide variety of neuronal markers, exhibit NMDA receptor-mediated intracellular calcium responses to agonists, and undergo excitotoxicity [11,14]. Differentiated P19 cells are most similar to human Nt-2N neurons, which are also derived from retinoic acid differentiation of teratocarcinoma precursor cells, express a wide variety of neuronal markers, and undergo NMDA receptor-mediated, hypoxia-induced excitotoxic cell death [25–28]. Our data demonstrated that our methods of differentiating P19 cells into neuron-like cells successfully result in the expression of NMDA receptors at the levels of mRNA, protein, MK-801 binding, MK-801-sensitive agonist-induced intracellular calcium responses, and MK-801-sensitive glutamate toxicity. Qualitatively, these data are in very good agreement with the literature, although quantitatively the MK-801 concentration required for rescue of the glutamate-challenged P19 cells was higher than what is typically observed in primary neuronal culture. However, the requirement for micromolar or greater concentrations of MK-801 to be effective has been observed in various other models of NMDA receptor-dependent glutamate toxicity and intracellular calcium responses, including reports from cerebellar granule neurons and NMDA receptor transfected HEK-293 cells [29–31]. Perhaps it is more difficult for MK-801 to achieve equilibrium under physiological conditions in these cell model systems due to differences in resting membrane potential or other cell-specific components that might affect channel activity. At the mRNA and protein levels, interestingly, we achieved reliable expression of the epsilon1 subunit of the NMDA receptor in addition to expression of zeta1 and epsilon2, which has not been achieved with other reported methods of P19 cell differentiation [32]. The presence of all three subunits more closely resembled expression patterns observed in adult rodent forebrain regions, including cortex and hippocampus [33]. It is also interesting to note that epsilon2 mRNA expression appeared to be transient (it peaked around 4 days after retinoic acid induction, and then disappeared by day 9), whereas protein levels were detected at a later stage of differentiation. These data might be indicative of developmentally regulated expression of the epsilon2 subunit in these cells, and warrant further investigation.

Our data demonstrated that glutamate toxicity in differentiated P19 cells requires NMDA receptor activation, since

the toxicity was completely blocked in the presence of the specific NMDA receptor antagonist MK-801. The requirement for glycine also suggests that NMDA rather than AMPA/kainate receptors is the primary mediator of toxicity. However, the data do not exclude the possibility that AMPA or kainate receptors may also be activated by glutamate and contribute to the excitotoxicity. This possibility would be consistent with data from primary neuronal culture, which reports that intracellular calcium responses to glutamate agonists involve multiple components [34]. Such components include AMPA/kainate receptor activation, membrane depolarization, voltage-gated calcium channel activation, relief of NMDA receptor magnesium block, and NMDA receptor activation. However, even with such a high level of complexity, in many primary neuronal models, glutamate excitotoxicity signals through the NMDA receptor and requires its activation to result in neuronal death [35], as was the case for differentiated P19 cells in this study.

Our data demonstrated that U0126, a MEK1/2 inhibitor, is protective against glutamate toxicity in differentiated P19 cells. U0126 exhibited a potency for protection against cell death, which closely matched its known potency for *in vitro* inhibition of wild-type MEK1/2 [15]. In addition, U0126 directly blocked glutamate-induced increases in ERK1/2 phosphorylation in the cells, but had no effect on NMDA receptor intracellular calcium responses or [^{3}H]MK-801 binding. These data suggest that the mechanism of U0126 cytoprotection is likely mediated through inhibition of MEK1/2. In contrast, several other classes of kinase inhibitors demonstrated very little or no neuroprotective efficacy, except for one p38 inhibitor compound, RWJ 68354. Unlike U0126, the p38 inhibitor potency for cytoprotection did not match its known potency for *in vitro* inhibition of p38 [16]. Moreover, other structurally unrelated p38 inhibitors showed no protective efficacy, suggesting that p38 MAP kinase inhibition is not a likely mechanism of protection against glutamate toxicity in differentiated P19 cells.

Evidence from the literature suggests that MEK inhibition is an effective neuroprotective strategy *in vivo* [7]. These reports indicate that transient cerebral ischemia induces p42 MAP kinase phosphorylation in rodent brain. A selective inhibitor of MEK1/2 can block this effect, and can reduce the extent of neuronal damage [7]. Primary neuronal culture also suggests that the p44/42 MAP kinase pathway is relevant to excitotoxic damage *in vitro* [9]. These reports indicate that glutamate signaling through its various ionotropic and/or metabotropic receptors results in p44/42 MAP kinase activation. Increased p44/42 MAP kinase activation induces immediate early gene transcription [36] and is implicated in seizure activity-induced cell death of cultured hippocampal neurons [9]. p44/42 MAP kinase activation also occurs in response to non-glutamate receptor-mediated neuronal oxidative injury, and contributes to this form of toxicity [10]. Our data suggest that in a neuron-like cell culture model system, NMDA receptor activation is linked to the p44/42 MAP kinase pathway, and that this downstream signaling pathway is critically involved in glutamate-induced toxicity.

U0126, but not RWJ 68354, was maximally protective even when added several hours after the onset of the glutamate challenge. This suggests that differentiated P19 cells undergoing glutamate-induced toxicity do not irreversibly commit to cell death until hours after the initial insult, but that this commitment is p42/44 MAP kinase pathway specific. This commitment could be a discreet signaling event that takes time to get activated, or could be the accumulation of intracellular signaling events that reach a threshold level of activation that commits the cell to die. This protracted process from receptor-mediated glutamate signal transduction to cell death commitment provides a window of time for intervention where components along this pathway can be blocked to prevent permanent neuronal damage. Using U0126, our studies indicate that MEK1/2 inhibition, but not p38 inhibition, can intervene in such a delayed fashion. U0126 inhibition of MEK, several hours after the glutamate challenge, may favor phosphatase dephosphorylation of p42 MAP kinase (ERK2), and restabilize this signaling pathway within enough time to prevent cell death. The concept of a compound that is able to exert delayed neuroprotection even when added after an ischemic event is an especially sought after property of a potential stroke therapeutic. Many compounds with diverse mechanisms are reported to exhibit post-treatment delayed neuroprotection. Among these are glutamate receptor antagonists [37], antioxidants [38], anticonvulsants [8,39], protease inhibitors [40], kinase inhibitors [10,41], and magnesium [42]. However, this is the first demonstration in a cell culture model of NMDA receptor-dependent glutamate toxicity that a specific inhibitor of the p44/42 MAP kinase pathway exhibits delayed neuroprotection. The window of time for efficacy is up to 6 hr after the onset of toxic challenge.

The signaling pathways that link the extracellular glutamate signal to p44/42 MAP kinase activation, or the downstream pathways that link p44/42 MAP kinase to delayed cytotoxicity are not well understood. The upstream activators of p44/42 (ERK1/2) MAP kinases are MEK1/2 [43]. MEK1/2 are phosphorylated by the Raf family of kinases [44], which are activated by the Ras family of small GTP-binding proteins [45]. One candidate intermediate molecule that may couple NMDA receptor activation to the Ras/Raf/MEK/ERK signaling cascade is the calcium-dependent tyrosine kinase PYK2 [46]. Increased intracellular calcium levels can activate PYK2, which can, in turn, activate MAP kinase signaling. A second candidate intermediate that may link ion channel activation to MAP kinase signaling is CaM-K. Two types of CaM-Ks are highly expressed in neurons, CaM-KII and CaM-KIV. These protein kinases are activated upon binding of calcium and calmodulin, and they can regulate p38, JNK, and ERK kinase activity [47]. However, in the case of neuronally differentiated P19 cells, CaM-Ks may not be such relevant signaling intermediates

between the NMDA receptor and the p44/42 (ERK1/2) MAP kinase pathway since KN-62, an inhibitor of CaM-Ks, does not prevent glutamate toxicity in these cells. A third candidate intermediate molecule may be NO. In cortical neurons, NMDA receptor coupling to NO production through PSD-95 is required for NMDA receptor-triggered neurotoxicity [48]. Increased NO production can also increase p44/42 MAP kinase activity [49]. Molecules that are downstream of p44/42 MAP kinase include transcription factors such as CREB, Elk-1, c-Jun, c-Fos, and NF-κB [50,51]. The p44/42 MAP kinase pathway can also induce phosphorylation of cytoskeletal components such as neurofilaments [52], regulate synapsin I-actin interactions [53], phosphorylate myelin basic protein [54], and regulate the secretion of amyloid precursor protein [55]. Therefore, there are many potential mediators of cytotoxicity downstream of p44/42 MAP kinase activation. Further investigation into whether any or all of these molecules are relevant is warranted.

A detailed understanding of the signaling pathways that are activated downstream of glutamate receptor stimulation is crucial for determining efficient means of preventing hypoxia/ischemia-induced neuronal damage. The present results suggest that in a cell culture model of glutamate toxicity, downstream signaling through the p44/42 MAP kinase pathway is a necessary component of glutamate-induced cell death. Based on these data, further investigation of the mechanistic relevance of this signaling pathway in glutamate excitotoxicity in primary neuronal culture and *in vivo* is warranted. Collectively, studies such as these may help demonstrate that inhibition of p44/42 MAP kinase signaling can be a useful protective strategy in the treatment of human neurological disease.

References

[1] Meldrum B, Garthwaite J. Excitatory amino acid neurotoxicity and neurodegenerative disease. Trends Pharmacol Sci 1990;11:379–87.

[2] Park CK, Nehls DG, Graham DI, Teasdale GM, McCulloch J. The glutamate antagonist MK-801 reduces focal ischemic brain damage in the rat. Ann Neurol 1988;24:543–51.

[3] Schneggenburger R, Zhou Z, Konnerth A, Neher E. Fractional contribution of calcium to the cation current through glutamate receptor channels. Neuron 1993;11:133–43.

[4] Bading H, Greenberg ME. Stimulation of protein tyrosine phosphorylation by NMDA receptor activation. Science 1991;253:912–4.

[5] Xia Z, Dickens M, Raingeaud J, Davis RJ, Greenberg ME. Opposing effects of ERK and JNK-p38 MAP kinases on apoptosis. Science 1995;270:1326–31.

[6] Yang DD, Kuan CY, Whitmarsh AJ, Rincon M, Zheng TS, Davis RJ, Rakic P, Flavell RA. Absence of excitotoxicity-induced apoptosis in the hippocampus of mice lacking the Jnk3 gene. Nature 1997;389:865–70.

[7] Alessandrini A, Namura S, Moskowitz M, Bonventre J. MEK1 protein kinase inhibition protects against damage resulting from focal cerebral ischemia. Proc Natl Acad Sci USA 1999;96:12866–9.

[8] Yang Y, Shuaib A, Li Q, Siddiqui M. Neuroprotection by delayed administration of topiramate in a model of middle cerebral artery embolization. Brain Res 1998;804:169–76.

[9] Murray B, Alessandrini A, Cole AJ, Yee AG, Furshpan EJ. Inhibition of the p44/42 MAP kinase pathway protects hippocampal neurons in a cell-culture model of seizure activity. Proc Natl Acad Sci USA 1998;95:11975–80.

[10] Stanciu M, Wang Y, Kentor R, Burke N, Watkins S, Kress G, Reynolds I, Klann E, Angiolieri M, Johnson J, DeFranco D. Persistent activation of ERK contributes to glutamate-induced oxidative toxicity in a neuronal cell line and primary cortical neuron cultures. J Biol Chem 2000;275:12200–6.

[11] Turetsky DM, Huettner JE, Gottlieb DI, Goldberg MP, Choi DW. Glutamate receptor-mediated currents and toxicity in embryonal carcinoma cells. J Neurobiol 1993;24:1157–69.

[12] McBurney MW, Rogers BJ. Isolation of male embryonal carcinoma cells and their chromosomal replication patterns. Dev Biol 1982;89:503–8.

[13] Jones-Velleneuve EMV, McBurney MW, Rogers KA, Kalnins VI. Retinoic acid induces embryonal carcinoma cells to differentiate into neurons and glial cells. J Cell Biol 1982;94:253–62.

[14] Grobin AC, Inglefield JR, Schwartz-Bloom RD, Devaud LL, Morrow AL. Fluorescence imaging of $GABA_A$ receptor-mediated intracellular [Cl^-] in P19-N cells reveals unique pharmacological properties. Brain Res 1999;827:1–11.

[15] Favata MF, Horiuchi KY, Manos EJ, Daulerio AJ, Stradley DA, Feeser WS, Van Dyk DE, Pitts WJ, Earl RA, Hobbs F, Copeland RA, Magolda RL, Scherle PA, Trzaskos JM. Identification of a novel inhibitor of mitogen-activated protein kinase kinase. J Biol Chem 1998;273:18623–32.

[16] Henry JR, Rupert KC, Dodd JH, Turchi IJ, Wadsworth SA, Cavender DE, Fahmy B, Olini GC, Davis JE, Pellegrino-Gensey JL, Schafer PH, Siekierka JJ. 6-Amino-2-(4-fluorophenyl)-4-methoxy-3-(4-pyridyl)-1*H*-pyrrolo[2,3-*b*]pyridine (RWJ 68354): a potent and selective p38 kinase inhibitor. J Med Chem 1998;41:4196–8.

[17] White MJ, DiCaprio MJ, Greenberg DA. Assessment of neuronal viability with Alamar blue in cortical and granule cell cultures. J Neurosci Methods 1996;70:195–200.

[18] Johnson J, Ascher P. Glycine potentiates the NMDA response in cultured mouse brain neurons. Nature 1987;325:529–31.

[19] Tokumitsu H, Chijiwa T, Hagiwara M, Mizutani A, Terasawa M, Hidaka H. KN-62, 1-[*N*,*O*-bis(5-isoquinolinesulfonyl)-*N*-methyl-l-tyrosyl]-4-phenylpiperazine, a specific inhibitor of Ca^{2+}/calmodulin-dependent protein kinase II. J Biol Chem 1990;265:4315–20.

[20] Kobayashi E, Nakano H, Morimoto M, Tamaoki T. Calphostin C (UCN-1028C), a novel microbial compound, is a highly potent and specific inhibitor of protein kinase C. Biochem Biophys Res Commun 1989;159:548–53.

[21] Onoda T, Iinuma H, Sasaki Y, Hamada M, Isshiki K, Naganawa H, Takeuchi T, Tatsuta K, Umezawa K. Isolation of a novel tyrosine kinase inhibitor, lavendustin A, from *Streptomyces griseolavendus*. J Nat Prod 1989;52:1252–7.

[22] Chijiwa T, Mishima A, Hagiwara M, Sano M, Hayashi K, Inoue T, Naito K, Toshioka T, Hidaka H. Inhibition of forskolin-induced neurite outgrowth and protein phosphorylation by a newly synthesized selective inhibitor of cyclic AMP-dependent protein kinase, *N*-[2-(*p*-bromocinnamylamino)ethyl]-5-isoquinolinesulfonamide (H-89), of PC12D pheochromocytoma cells. J Biol Chem 1990;265:5267–72.

[23] Lee J, Laydon J, McDonnell P, Gallagher T, Kumar S, Green D, McNulty D, Blumenthal M, Heys J, Landvatter S. A protein kinase involved in the regulation of inflammatory cytokine biosynthesis. Nature 1994;372:739–46.

[24] Inhorn RC, Majerus PW. Inositol polyphosphate 1-phosphatase from calf brain. Purification and inhibition by Li^+, Ca^{2+}, and Mn^{2+}. J Biol Chem 1987;262:15946–52.

[25] Pleasure SJ, Page C, Lee V-M. Pure, postmitotic, polarized human neurons derived from NTera 2 cells provide a system for expressing exogenous proteins in terminally differentiated neurons. J Neurosci 1992;12:1802–15.

[26] Younkin DP, Tang C-M, Hardy M, Reddy UR, Shi Q-Y, Pleasure SJ, Lee V-M, Pleasure D. Inducible expression of neuronal glutamate receptor channels in the NT2 human cell line. Proc Natl Acad Sci USA 1993;90:2174–8.
[27] Munir M, Lu L, McGonigle P. Excitotoxic cell death and delayed rescue in human neurons derived from NT2 cells. J Neurosci 1995; 15:7847–60.
[28] Rootwelt T, Dunn M, Yudkoff M, Itoh T, Almaas R, Pleasure D. Hypoxic cell death in human NT2-N neurons: involvement of NMDA and non-NMDA glutamate receptors. J Neurochem 1998;71:1544–53.
[29] Perrier ML, Benavides J. Pharmacological heterogeneity of NMDA receptors in cerebellar granule cells in immature rat slices. A microfluorimetic study with the $[Ca^{2+}]_i$ sensitive dye Indo-1. Neuropharmacology 1995;34:35–42.
[30] Anegawa NJ, Lynch DR, Verdoorn TA, Pritchett DB. Transfection of *N*-methyl-D-aspartate receptors in a nonneuronal cell line leads to cell death. J Neurochem 1995;64:2004–12.
[31] Grant E, Bacskai B, Pleasure D, Pritchett D, Gallagher M, Kendrick S, Kricka L, Lynch D. *N*-Methyl-D-aspartate receptors expressed in a non-neuronal cell line mediate subunit-specific increases in free intracellular calcium. J Biol Chem 1997;272:647–56.
[32] Ray WJ, Gottlieb DI. Expression of ionotropic glutamate receptor genes by P19 embryonal carcinoma cells. Biochem Biophys Res Commun 1993;197:1475–82.
[33] Monyer H, Burnashev H, Laurie D, Sakmann B, Seeburg P. Developmental and regional expression in the rat brain and functional properties of four NMDA receptors. Neuron 1994;12:529–40.
[34] Courtney M, Lambert J, Nicholls D. The interactions between plasma membrane depolarization and glutamate receptor activation in the regulation of cytoplasmic free calcium in cultured cerebellar granule cells. J Neurosci 1990;10:3873–9.
[35] Tymianski M, Charlton M, Carlen P, Tator C. Source specificity of early calcium neurotoxicity in cultured embryonic spinal neurons. J Neurosci 1993;13:2085–104.
[36] Xia Z, Dudek H, Miranti CK, Greenberg ME. Calcium influx via the NMDA receptor induces immediate early gene transcription by a MAP kinase/ERK-dependent mechanism. J Neurosci 1996;16:5425–36.
[37] Li MM, Payne RS, Reid KH, Tseng MT, Rigor BM, Schurr A. Correlates of delayed neuronal damage and neuroprotection in a rat model of cardiac-arrest-induced cerebral ischemia. Brain Res 1999; 826:44–52.
[38] Sakakibara Y, Mitha AP, Ogilvy CS, Maynard KI. Post-treatment with nicotinamide (vitamin B_3) reduces the infarct volume following permanent focal cerebral ischemia in female Sprague-Dawley and Wistar rats. Neurosci Lett 2000;281:111–4.
[39] Wasterlain C, Adams L, Wichmann J, Sofia R. Felbamate protects CA1 neurons from apoptosis in a gerbil model of global ischemia. Stroke 1996;27:1236–40.
[40] Cheng Y, Deshmukh M, D'Costa A, Emaro J, Gidday J, Shah A, Jacquin M, Johnson E, Holtzman D. Caspase inhibitor affords neuroprotection with delayed administration in a rat model of neonatal hypoxic-ischemic brain injury. J Clin Invest 1998;101:1992–9.
[41] Tatlisumak T, Takano K, Carano R, Miller L, Foster A, Fisher M. Delayed treatment with an adenosine kinase inhibitor, GP683, attenuates infarct size in rats with temporary middle cerebral artery occlusion. Stroke 1998;29:1952–8.
[42] Heath D, Vink R. Improved motor outcome in response to magnesium therapy received up to 24 hours after traumatic diffuse axonal brain injury in rats. J Neurosurg 1999;90:504–9.
[43] Anderson N, Maller J, Tonks N, Sturgill T. Requirement for integration of signals from two distinct phosphorylation pathways for activation of MAP kinase. Nature 1990;343:651–3.
[44] Moodie SA, Willumsen BM, Weber MJ, Wolfman A. Complexes of Ras·GTP with Raf-1 and mitogen-activated protein kinase kinase. Science 1993;260:1658–61.
[45] Papin C, Eychene A, Brunet A, Pages G, Pouyssegur J, Calothy G, Barnier JV. B-Raf protein isoforms interact with and phosphorylate Mek-1 on serine residues 218 and 222. Oncogene 1995;10:1647–51.
[46] Lev S, Moreno H, Martinez R, Canoll P, Peles E, Musacchio JM, Plowman GD, Rudy B, Schlessinger J. Protein tyrosine kinase PYK2 involved in Ca^{2+}-induced regulation of ion channel and MAP kinase functions. Nature 1995;376:737–45.
[47] Enslen H, Tokumitsu H, Stork P, Davis R, Soderling T. Regulation of mitogen-activated protein kinases by a calcium/calmodulin-dependent protein kinase cascade. Proc Natl Acad Sci USA 1996;93: 10803–8.
[48] Sattler R, Xiong Z, Lu W, Hafner M, MacDonald J, Tymianski M. Specific coupling of NMDA receptor activation to nitric oxide neurotoxicity by PSD-95 protein. Science 1999;284:1845–8.
[49] Lander H, Jacovina A, Davis R, Tauras J. Differential activation of mitogen-activated protein kinases by nitric oxide-related species. J Biol Chem 1996;271:19705–9.
[50] Vanhoutte P, Barnier L-V, Guibert B, Pages C, Besson M-J, Hipskind R, Caboche J. Glutamate induces phosphorylation of Elk-1 and CREB, along with c-fos activation, via an extracellular signal-regulated kinase-dependent pathway in brain slices. Mol Cell Biol 1999; 19:136–46.
[51] Ryan KM, Ernst MK, Rice NR, Vousden KH. Role of NF-κB in p53-mediated programmed cell death. Nature 2000;404:892–7.
[52] Li BS, Veeranna, Gu J, Grant P, Pant HC. Activation of mitogen-activated protein kinases (Erk1 and Erk2) cascade results in phosphorylation of NF-M tail domains in transfected NIH 3T3 cells. Eur J Biochem 1999;262:211–7.
[53] Jovanovic J, Benfenati F, Siow Y, Sihra T, Sanghera J, Pelech S, Greengard P, Czernik A. Neurotrophins stimulate phosphorylation of synapsin I by MAP kinase and regulate synapsin I-actin interactions. Proc Natl Acad Sci USA 1996;93:3679–83.
[54] Ahn N, Seger R, Bratlien R, Diltz C, Tonks N, Krebs E. Multiple components in an epidermal growth factor-stimulated protein kinase cascade. *In vitro* activation of a myelin basic protein/microtubule-associated protein 2 kinase. J Biol Chem 1991;266:4220–7.
[55] Desdouits-Magnen J, Desdouits F, Takeda S, Syu L, Saltiel A, Buxbaum J, Czernik A, Nairn A, Greengard P. Regulation of secretion of Alzheimer amyloid precursor protein by the mitogen-activated protein kinase cascade. J Neurochem 1998;70:524–30.